Accepted Manuscript

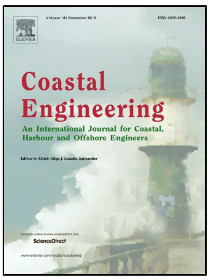

Physical modelling of local scour at twin piles under combined waves and current

Wen-Gang Qi, Yi-Xuan Li, Kai Xu, Fu-Ping Gao

PII:	S0378-3839(18)30526-X
DOI:	10.1016/j.coastaleng.2018.10.009
Reference:	CENG 3437
To appear in:	*Coastal Engineering*
Received Date:	21 October 2017
Accepted Date:	27 October 2018

Please cite this article as: Wen-Gang Qi, Yi-Xuan Li, Kai Xu, Fu-Ping Gao, Physical modelling of local scour at twin piles under combined waves and current, *Coastal Engineering* (2018), doi: 10.1016/j.coastaleng.2018.10.009

Outline

Physical modelling of local scour at twin piles under combined waves and current

Wen-Gang Qi [a,b], Yi-Xuan Li [a,b,c], Kai Xu [a,b], Fu-Ping Gao [a,b,*]

[a] *Key Laboratory for Mechanics in Fluid Solid Coupling Systems, Institute of Mechanics, Chinese Academy of Sciences, Beijing 100190, China*

[b] *School of Engineering Science, University of Chinese Academy of Sciences, Beijing 100049, China*

[c] *Civil Infrastructure Operations Dept., China State Construction Engineering Corp. Ltd., Beijing 100044, China*

ABSTRACT

Under the actions of ocean waves and current, severe local scour can be induced around pile groups, significantly compromising the safety of marine structures. A series of flume tests were conducted for physical modelling the local scouring process around twin piles in the cohesionless soils under combined waves and currents, and compared with the pure current case. The effects of non-dimensional pile spacing (G/D) and flow skew angle (α) on the scour depth and time scale of scour around twin piles are intensively examined. The experimental observations indicate that the influence of pile spacing on the scour depth development is much more significant for the side-by-side ($\alpha=90^o$) arrangement than that for the tandem arrangement ($\alpha=0^o$). With the increase of flow skew angle α, the maximum scour depth is remarkably enhanced within the examined range $0 \le G/D \le 3.0$. When G/D=3.0, the pile group effect on the time scale is generally negligible for pure current cases, whereas a prominent pile-group effect can still be observed for combined wave-current cases, especially for the side-by-side arrangement. A parameter of "equivalent pile diameter" is then introduced for evaluating the maximum scour depth at the twin piles with the previous formulas for the single pile. Based on the existing and present experimental data, the empirical formula of dimensionless equivalent pile diameter as the function of G/D and α is established to predict the maximum scour depth at the twin piles.

Keywords: local scour; twin piles; pile-group; skew angle; horseshoe vortex; PIV technique; combined waves and current; time scale; equivalent pile diameter

* Corresponding author. Tel:+86 10 82544189, Fax:+86 10 62561284

E-mail address: fpgao@imech.ac.cn (Fu-Ping Gao)

This revised version is submitted to ***Coastal Engineering*** for review

1. Introduction

Pile groups are widely used in offshore and/or coastal engineering practice to support offshore oil and gas platforms and marine transportation systems (e.g. piers, jetties and cross-sea bridges). The safety of offshore piles in sand could be significantly compromised by waves/current-induced scour. It is of great significance to understand the scouring process around a group of vertical piles. While a substantial amount of knowledge has accumulated about scour around a single pile over the past half century (Sumer and Fredsøe, 2002; Whitehouse, 1998; Chiew and Melville, 1987; Larsen et al., 2017), the pile-group effects on the local scour still need to be further studied.

The assessment of the scour depth is crucial in the design of the foundation for structures. The scour around group of piles in regular waves was investigated in laboratory tests by Sumer and Fredsøe (1998). The dimensions of the scour hole were found to be affected by the pile spacing and the orientation of the piles. The interference between the piles becomes increasingly important as the pile spacing decreases. The pile group behaves as a single body for small values of the pile spacing. Field studies were later reported by Bayram and Larson (2000) for scour around a group of piles under waves. The field observations indicate that the maximum scour depth has a distinct correlation with the Keulegan-Carpenter number, which is quite similar to the laboratory data obtained by Sumer et al. (1992b). Twin piles are an elementary unit for pile groups. Liang et al. (2013) investigated the scour around twin piles subjected to oscillatory flows, and found that the individual piles in twin piles behave independently when the pile spacing is three times greater than the pile diameter. The pile height effect was also examined and an empirical formula was proposed to describe the reduction of scour depth with pile height. For the random wave scour around group of slender piles, Myrhaug and Rue (2005) proposed a tentative approach to derive the scour depth.

For conditions of steady current, Ataie-Ashtiani and Beheshti (2006) carried out a series of experiments covering different pile group arrangements, spacing and flow speed, and a correction factor was derived to

predict the maximum scour depth for the pile groups. A series of flume tests were performed by Wang et al. (2016) to investigate the characteristics of local scour at twin piles in a tandem arrangement under clear-water conditions. It was observed that the scour depth at the rear pile was less than that at the front pile due to the sheltering effects. Kim et al. (2014) numerically studied the local scour development around twin piles in a side-by-side or tandem arrangement under clear-water conditions. The features of scour development and bed topography in the equilibrium state were interpreted based on the flow field around cylinders. The results of the maximum scour depths between the simulations and the measured data reported by Ataie-Ashitian and Beheshti (2006) are consistent.

The available experimental studies have contributed to enhance the knowledge about the pile-group effects on the local scour. In comparison, the flow field around pile groups, which is the inducement of the development of local scour, has not been well understood. Moreover, for the scour around pile groups under combined waves and current, which is a common scenario in marine environments, it appears that few experimental studies can be found.

In this paper, a series of scour tests around twin piles were conducted in a water flume. The layout of twin piles is usually a portion of a larger pile group. The understanding of the physics of local scour around twin piles is fundamental to the general understanding of scour around more complex pile groups. Two different hydrodynamic conditions, i.e., pure current and combined waves and current (waves propagating along current direction), were examined. The pile-group effects on the local scour around twin piles are compared in reference to different hydrodynamic conditions and layouts. The flow measurements around twin piles under pure current were complementally carried out using PIV technique, and the results were analyzed to physically explain the pile-group effects on local scour.

2. Physical modelling methods

2.1. Experimental set-up

The tests were conducted in a flow-structure-soil interaction flume (52.0 m long, 1.0 m wide and 1.5 m high). The flume can generate a constant flow and waves concurrently. A saturated sand-bed was prepared to simulate a sandy seabed, which is 0.5 m thick and 6.0 m long (see Fig. 1). The water depth h was kept constant at 0.5 m. The main physical properties of sand-bed are: mean size of sand grains d_{50}=0.15 mm, geometric standard deviation of soil grains $\sigma_g = 1.65$, soil porosity n=0.35, relative density D_r=0.62 and submerged unit weight of soil γ'=10.65 kN/m^3.

As illustrated in Fig. 1, the far-field wave height was measured with a wave height gauge along the central line at the distance of 15 m apart from the front pile. An Acoustic Doppler Velocimetry (ADV) was mounted to measure the undisturbed flow velocity at the level of 1.0D above the sand-bed at the distance of 20 m apart from the front pile center. The scour depth evolutions at upstream and downstream of each pile were monitored with four ultrasonic distance sensors.

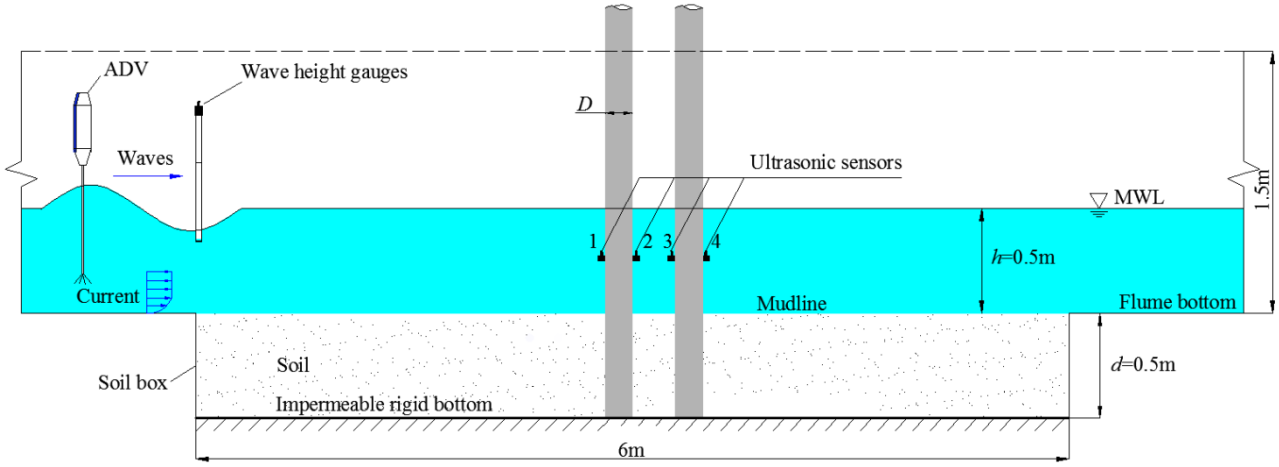

Fig. 1. Schematic diagram of scour tests for twin piles.

To enhance the understanding of the physical mechanism for local scour around twin piles, a PIV measurement was employed to capture the characteristics of the flow field around piles. At the test section, the bottom of flume is replaced with a piece of 1.0 m × 1.0 m transparent glass installed 16.0 m downstream of the flow inlet, as shown in Fig. 2. Through the transparent glass, double-pulsed laser sheets generated by a

LaVision PIV system illuminate the flow field around the piles from the bottom side. The camera was located outside the flume test section's side bottom. The time between exposures for image pairs was varied from test case to test case (for more details, refer to Anderson and Lynch, 2016).

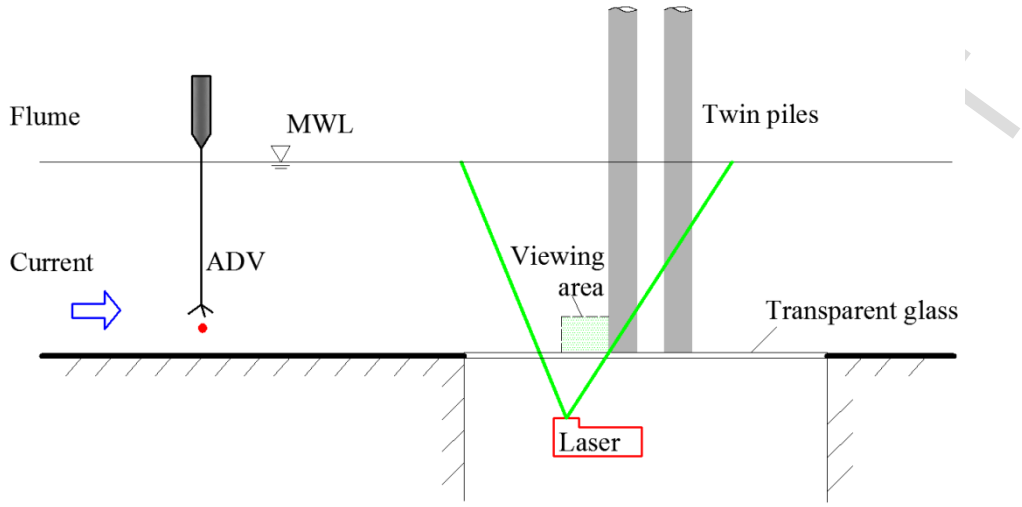

Fig.2. Sketch of PIV set-up for twin piles

The flow around the base of a vertical pile generally consists of two fundamental structures: horseshoe vortex (HSV) and wake vortices (Sumer et al., 1997). Under the conditions of pure current and combined waves and current, the scouring process is mainly controlled by the HSV (Qi and Gao, 2014a). Therefore, the present PIV tests mainly focus on the flow visualization of the HSV in front of piles.

The HSV around a pile is usually confined to a very limited space at the upstream junction corner (Kirkil and Constantinescu, 2015). The PIV viewing area was thus chosen at 100×75 mm (i.e. 0.833×0.625 *D*) in the *x*-*y* plane, yielding an image of resolution approximately 72.5 μm/pixel. Processing of the data was performed using LaVision Inc.'s DaVis 7.2 software. Particle image velocimetry velocity vectors were obtained by cross-correlation of the image pairs. An interrogation window size of 64×64 pixels with an overlapping of 50% was used. The resulting velocity vector fields for each image pair contained approximately 43×32 velocity vectors (*u*, *v*) with a vector spacing (spatial resolution) of approximately 2.33×2.33 mm. For each PIV test case, a total of 300 image pairs were acquired at a sampling rate of 4.75 Hz

(i.e. 63.16 s recordings), then averaged temporally to reflect the time-average characteristics of the flow field around twin piles. The free stream velocity 3.0 m upstream of the twin piles model was measured using acoustic Doppler velocimetry (ADV).

The magnitude of swirling strength (Chong et al., 1990), which can discriminate between vortices and shear motions successfully, is applied to qualify the intensity of the HSV at the upstream corner of piles in this study. The definition of swirling strength is related to the discriminant of complex eigenvalues of the local velocity gradient tensor. More details about the definition of swirling strength could refer to Zang et al. (2013).

2.2. Test conditions

Two pairs of plexiglass model piles (outer diameter of D=12.0 cm and D=8.0 cm) were adopted in the scour tests. As illustrated in Fig. 3, the twin piles were tested at four different flow skew angles (α=0°, 30°, 60°, 90°). The distance between the two piles was varied, with the gap-to-diameter ratio, G/D, ranging from 0 to 3.0. Note that the piles of D=12.0 cm were adopted for α=0° and 30° while the piles of D=8.0 cm were adopted for α=60° and 90°, to minimize the blockage effect. Two hydrodynamic conditions, i.e., pure current and combined waves and current, were adopted in the tests.

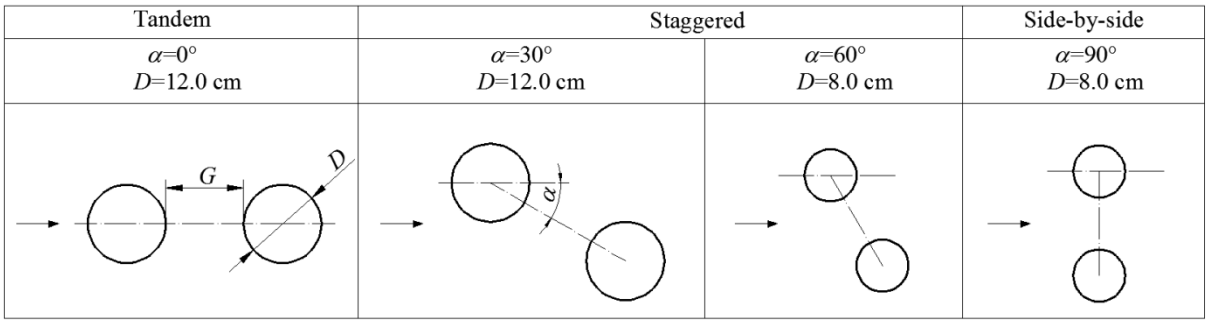

Fig. 3. Layout of twin piles for scour tests

Test conditions and measured maximum scour depths at twin piles are summarized in Table 1 for pure current, and Table 2 for combined waves and current. The wave parameters for the cases under combined waves and current are: wave height H=0.14 m and wave period T=1.8 s. As a reference, scour around a single pile was also tested. The data of scour around a single pile with D=8.0 cm under combined waves and current is missing due to an unexpected crash of the storage disk. To obtain the ratio of the maximum scour depth around twin piles (S) to that around a single pile (S_0) for the cases with D=8.0 cm under combined waves and current, the corresponding S_0 was estimated to be 7.4 cm based on the empirical prediction formula proposed by Qi and Gao (2014a). This value of S_0 is approximately equal to that under the condition of α=0 and G=3.0 (S_0=7.8 cm, see run 27 in Table 2). The analyses in Section 3.2 indicate that the pile-group effect generally vanishes for $G/D\geq$3.0. Therefore, the estimated value of S_0=7.4 cm for the cases with D=8.0 cm under combined waves and current is considered to be reasonable.

The quantities U_c and U_{wm} in Tables 1 and 2 are individually the velocity of the current component and orbital component of the undisturbed flow, measured at the level of 1.0D above the sand-bed, representing the characteristic flow velocity at the boundary layer. The pile Reynolds number (Re) is defined as

$$Re=U_m D/\nu \tag{1}$$

in which U_m ($=U_c+U_{wm}$) is the maximum value of the combined waves and current velocity at the level of 1.0D above the sand-bed and ν is the kinematic viscosity of water.

The pile Froude number (Fr) is defined as

$$Fr = U_c \Big/ \sqrt{gD} \tag{2}$$

The average-velocity based pile Froude number (Fr_a) is defined as (see Qi and Gao, 2014a)

$$Fr_a = U_a \Big/ \sqrt{gD} \tag{3}$$

in which U_a ($=\frac{1}{T/4}\int_0^{T/4}(U_c+U_{wm}\sin(2\pi t/T))dt=U_c+\frac{2}{\pi}U_{wm}$) is the average water particle velocity during one-quarter cycle of oscillation under combined waves and current, when the oscillatory motion and the current are in the

same direction; and g is the gravitational acceleration.

The Keulegan-Carpenter number (KC) is defined as

$$KC=U_{wm}T/D \tag{4}$$

The Shields parameter (θ) is defined as

$$\theta=\frac{U_f^2}{g(\rho_s/\rho_w-1)d_{50}} \tag{5}$$

in which U_f is the maximum value of the undisturbed friction velocity, ρ_s is the sediment grain density and ρ_w is the water density. The detailed calculation procedure of θ is given by Soulsby (1997). The critical Shields parameter coinciding with sediment motion can be calculated by (Soulsby, 1997)

$$\theta_{cr}=\frac{0.3}{1+1.2D_*}+0.055\left[1-\exp\left(-0.02D_*\right)\right] \tag{6}$$

in which $D_*=d_{50}[(s-1)g/\nu^2]^{1/3}$ is known as the dimensionless grain size and s is the specific gravity of sand grains. For the present examined sand-bed, the value of θ_{cr} is 0.058. As shown in Table 1 and 2, the clear-water scour regime prevailed for pure current conditions ($\theta<\theta_{cr}$), while the live-bed scour regime prevailed for the condition of combined waves and current ($\theta\geq\theta_{cr}$).

With respect to the scour around a single pile, a previous study has indicated that the effect of superimposing waves on a current is significant only when the sandy seabed is in the clear-water regime under pure current (Qi and Gao, 2014b). That is, the wave-induced transition from clear-water regime under pure current to live-bed regime under combined waves and current, is crucial to the difference of scouring process around a single pile. A primary concern of the present study is to investigate the difference of scouring process around twin piles between pure current cases and combined wave-current cases. Inferring from the aforementioned results for single pile cases, remarkably different scouring process can be reasonably anticipated only if the pure current cases are in clear water regime. Therefore, the current velocity is set as U_c=0.23 m/s to make pure current cases in clear-water regime and combined wave-current cases in live-bed regime for the present tests.

No sediment nourishment was provided upstream of the test section, implying a net outflow of sediments from the 6.0 m long test pit under live-bed condition (combined waves and current). To qualitatively evaluate the effect of sediments net outflow on the scour depth development, all the sand washed out of the test pit in runs 15 and 25 was carefully collected after the tests. The volumes of the collected sand were 11.23 litres (12.86 litres) in run 15 (run 25). Correspondingly, the general lowering of the sand bed level due to the sediments net outflow was about 1.87mm (2.14 mm) in run 15 (run 25). The durations of run 15 and run 25 are all approximately 2 h. Thus the sediments net outflow from the test pit made a contribution to the scouring rate by 0.94mm/h (1.07 mm/h) in run 15 (run 25), which can be considered negligible compared with the relatively rapid scouring rate under the corresponding live-bed condition.

Table 1. Test results for local scour around twin piles: Pure current

Run number	Pile layout	D (cm)	U_c (m/s)	θ	Re	Fr	S (cm)	S/S_0
1	Single pile	12.0	0.23	0.031	2.76×10^4	0.212	8.0	1.00
2	Single pile	8.0	0.23	0.031	1.84×10^4	0.260	7.0	1.00
3	α=0° G/D=0	12.0	0.23	0.031	2.76×10^4	0.212	6.8	0.85
4	α=0° G/D=1.0	12.0	0.23	0.031	2.76×10^4	0.212	8.6	1.08
5	α=30° G/D=0	12.0	0.23	0.031	2.76×10^4	0.212	10.7	1.34
6	α=30° G/D=1.0	12.0	0.23	0.031	2.76×10^4	0.212	8.4	1.05
7	α=30° G/D=3.0	12.0	0.23	0.031	2.76×10^4	0.212	8.5	1.06
8	α=60° G/D=0	8.0	0.23	0.031	1.84×10^4	0.260	9.0	1.29
9	α=60° G/D=0	8.0	0.23	0.031	1.84×10^4	0.260	11.2	1.60
10	α=60° G/D=1.0	8.0	0.23	0.031	1.84×10^4	0.260	8.3	1.19
11	α=60° G/D=3.0	8.0	0.23	0.031	1.84×10^4	0.260	8.2	1.17
12	α=90° G/D=0	8.0	0.23	0.031	1.84×10^4	0.260	12.5	1.78
13	α=90° G/D=1.0	8.0	0.23	0.031	1.84×10^4	0.260	9.0	1.29
14	α=90° G/D=3.0	8.0	0.23	0.031	1.84×10^4	0.260	7.5	1.07

Table 2. Test results for local scour around twin piles: Current with following waves

Run number	Pile layout	D (cm)	U_c (m/s)	U_{wm} (m/s)	θ	KC	Re	Fr_a	S (cm)	S/S_0
15	Single pile	12.0	0.23	0.25	0.409	3.75	5.76×10^4	0.362	9.8	1.00
16	α=0° G/D=0	12.0	0.23	0.25	0.409	3.75	5.76×10^4	0.362	9.2	0.94
17	α=0° G/D=1.0	12.0	0.23	0.25	0.409	3.75	5.76×10^4	0.362	9.5	0.97

18		*G/D*=0	12.0	0.23	0.25	0.409	3.75	5.76×10^4	0.362	13.2	1.35
19		*G/D*=1.0	12.0	0.23	0.25	0.409	3.75	5.76×10^4	0.362	10.2	1.04
20	*α*=30°	*G/D*=3.0	12.0	0.23	0.25	0.409	3.75	5.76×10^4	0.362	10.0	1.02
21		*G/D*=0	8.0	0.23	0.25	0.409	5.63	3.84×10^4	0.434	12.3	1.67
22		*G/D*=0	8.0	0.23	0.25	0.409	5.63	3.84×10^4	0.434	14.0	1.91
23	*α*=60°	*G/D*=1.0	8.0	0.23	0.25	0.409	5.63	3.84×10^4	0.434	11.0	1.50
24		*G/D*=3.0	8.0	0.23	0.25	0.409	5.63	3.84×10^4	0.434	8.5	1.16
25		*G/D*=0	8.0	0.23	0.25	0.409	5.63	3.84×10^4	0.434	15.2	2.07
26	*α*=90°	*G/D*=1.0	8.0	0.23	0.25	0.409	5.63	3.84×10^4	0.434	12.0	1.63
27		*G/D*=3.0	8.0	0.23	0.25	0.409	5.63	3.84×10^4	0.434	7.8	1.06

A pair of plexiglass model piles with D=12.0 cm were adopted in the PIV tests. The flow measurements were carried out under pure current with various types of piles layout (α = 0°, 30°, 60° and 90°; G/D=0 and 1.0), as shown in Fig. 4. The vertical stagnation planes for piles were examined, and the locations of the measurements are indicated with lines crossed by slashes in Fig. 4. The free stream velocity was kept constant at 0.23 m/s (measured at the level of 1.0D above the sand-bed).

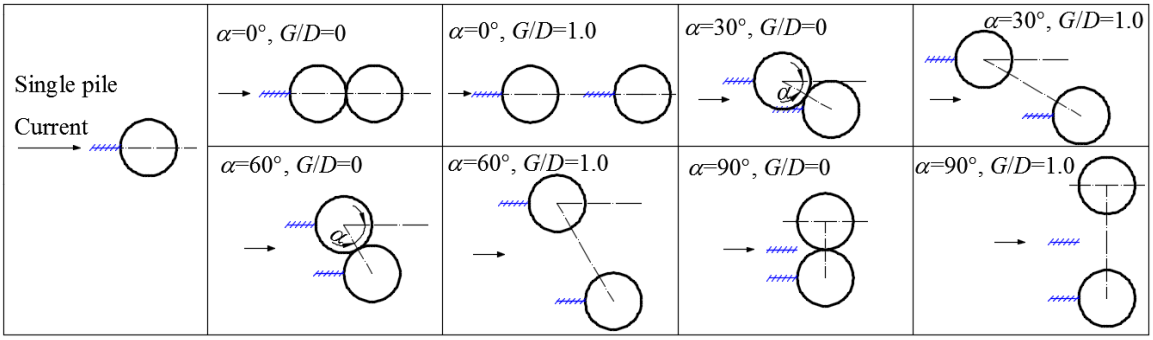

Fig. 4. Layout of single pile and twin piles for PIV tests

As a reference, the time-averaged field of flow velocity and swirling strength at the upstream corner of a single pile under pure current is measured and shown in Fig. 5. The single pile can also be considered as an extreme configuration of twin piles with the spacing between two piles being sufficiently large. Fig. 5 shows that the HSV can be easily identified either from flow velocity or swirling strength field. The position of the vortex center can be characterized by the longitudinal and vertical coordinates (λ_0 and ξ_v) with the intersection point between the upstream pile edge and the bed surface being set as the origin. Generally

constant values of λ_0/D ($\lambda_0/D=0.15\rightarrow0.25$ for Re=$5\times10^3\rightarrow3.5\times10^5$) and ξ_v/D ($\xi_v/D=0.028\rightarrow0.073$ for Re=$1\times10^3\rightarrow3.5\times10^5$) have been widely confirmed by both experimental and numerical results (Ballio et al., 1998; Qi et al., 2016). As shown in Fig. 5, the position of the HSV center corresponds to $\lambda_0/D=0.17$ and $\xi_v/D=0.054$, which is consistent with the existing results. The maximum swirling strength Ω_{max} locating at the core of the vortex is Ω_{max}=486 s^{-1}. Note that the value of Ω_{max} shown in Fig. 5 is a temporally averaged results according to 300 sequential image pairs. Due to the instantaneous oscillation of the HSV, the temporally averaged value of Ω_{max}=486 s^{-1} is significantly lower than the instantaneous one (approximately up to 2000 s^{-1} for the case of a single pile).

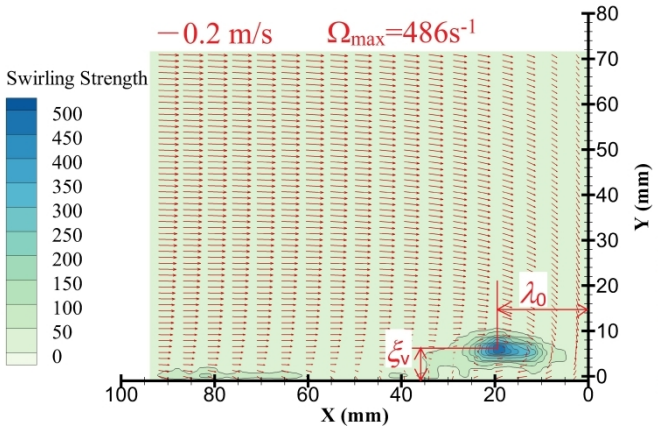

Fig. 5. Time-averaged fields of flow velocity and swirling strength at the upstream corner of a single pile (D=12.0 cm, U_c=0.23 m/s).

3. Experimental Results and Analyses

3.1. Local scour development at the twin piles

3.1.1 Tandem arrangements

Figs. 6 gives two series of scour depth developments at the upstream edge of the front model pile under pure current and the combined waves and current for tandem arrangement, demonstrating the effect of pile spacing. It is indicated that the scour depths for all the cases in Fig. 6 experience a rapid increase at the

beginning. Thereafter, the scour depths tend to approach equilibrium state with a significant reduction of increasing rate of the scour depth. It is noted that none of the tests in Fig. 6 (also see Figs. 8 and 12) have reached the equilibrium stage, especially for the cases under pure current where clear-water condition prevails. The results of Yagci et al. (2017) suggest that the clear-water scour depth achieved at 2 hours may be as small as a factor 1.5 compared to that obtained at the end of 8 hours. Melville and Chiew (1999) reported that in order to achieve equilibrium scour depth under clear-water condition in small-scale laboratory experiments, it was necessary to conduct experiment for several days. However, the primary focus of this study is a comparison of the scour depth and corresponding flow mechanism between different configurations of twin piles rather than the exact value of equilibrium scour depth, such that a test duration of 120 minutes should be sufficient for the present scope of the study.

Fig. 6 shows that the maximum scour depth at the front pile for the tandem arrangements is smaller than the single pile cases under either pure current or combined waves and current. Moreover, for the cases under pure current with relatively small spacing (i.e. G/D=0 and 1.0), the scour depths develop more tardily compared with the cases of single pile. This should be attributed to the enlarged dimension of the scour hole along the flow direction for the cases with G/D=0 and 1.0. Due to the relatively small spacing, two local scour holes around the front pile and the rear pile merged into one and the path for a sand particle to move out of the merged scour hole became longer.

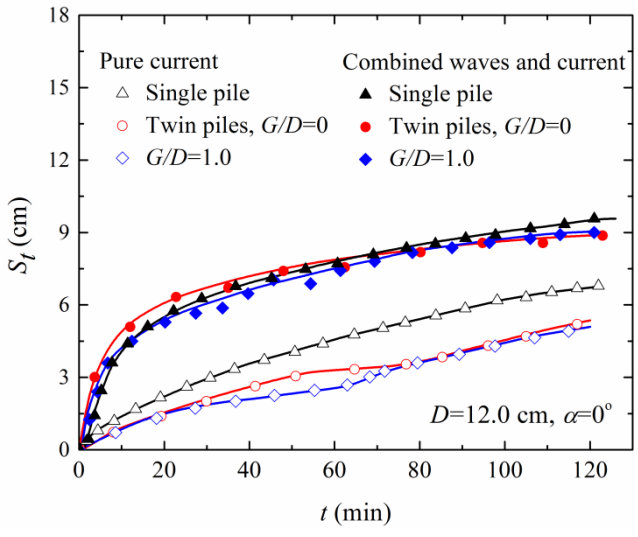

Fig. 6. Time development of scour depth measured at upstream edge of the front pile with various pile spacings for tandem arrangement (pure current: runs 1 3, & 4; combined waves and current: runs 15, 16 & 17).

The time-averaged fields of flow velocity and swirling strength at the upstream corner of twin piles with tandem arrangements (*G/D*=0 and *G/D*=1.0) are indicated in Fig. 7. The size of the vortex can be clearly observed and the maximum swirling strength is given, which can indicate the strength of the HSV comprehensively (Muzzammil and Gangadhariah, 2003). Fig. 7 shows that the size of the HSV at the front pile generally remains the same as the single pile case. Nevertheless, the values of the maximum swirling strength for tandem arrangements are significantly lower than the single pile case, which could be partially responsible for the reduced maximum scour depth for tandem arrangements compared to the single pile case. Fig. 7(c) indicates that no HSV forms around the rear pile for tandem arrangement with *G/D*=1.0, due to the significant sheltering effect from the front pile. The irregular distribution of swirling strength results from the lee side wake vortices from the front pile.

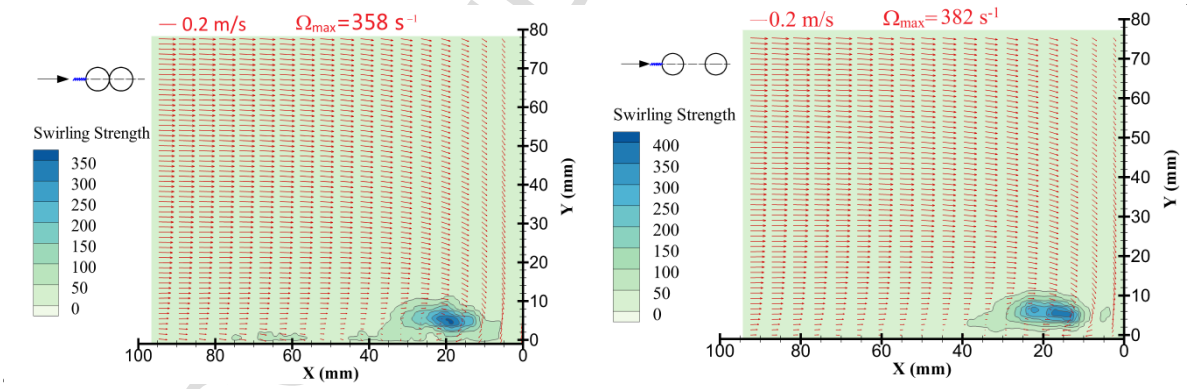

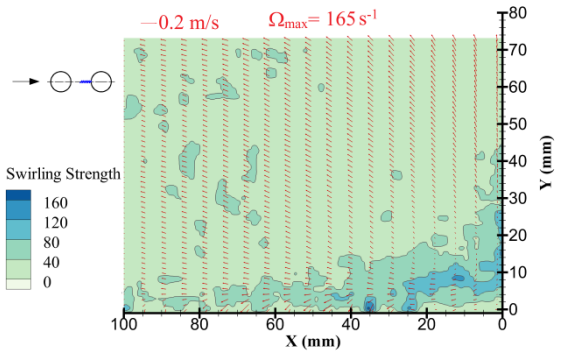

(c)

Fig. 7. Time-averaged fields of flow velocity and swirling strength at the upstream corner of twin piles: (a) front pile, $\alpha = 0^o$, G/D=0; (b) front pile, $\alpha = 0^o$, G/D=1.0; and (c) rear pile, $\alpha = 0^o$, G/D=1.0.

3.1.2 Staggered arrangements

The developments of scour depth at the upstream edge of the front pile with various pile spacings for staggered arrangements are shown in Fig. 8. The pile diameter adopted in the cases with α=30^o is D=12cm while in the cases with α=60^o is D=8cm to avoid the blockage effect. A comparison of the scour holes around the twin piles under combined waves and current with α=30° and G/D=1.0, 2.0, 3.0 is shown in Fig. 9. In contrast to the cases with tandem arrangement, the rate of scour depth for staggered cases with G/D=0 is remarkably faster than that for single pile. Nevertheless, the rate of scour depth for G/D =1.0 and 3.0 is generally consistent with and even slightly slower than that for single pile. The effects of pile spacing on the development of scour depth are the same for the cases with pure current and cases with combined waves and current.

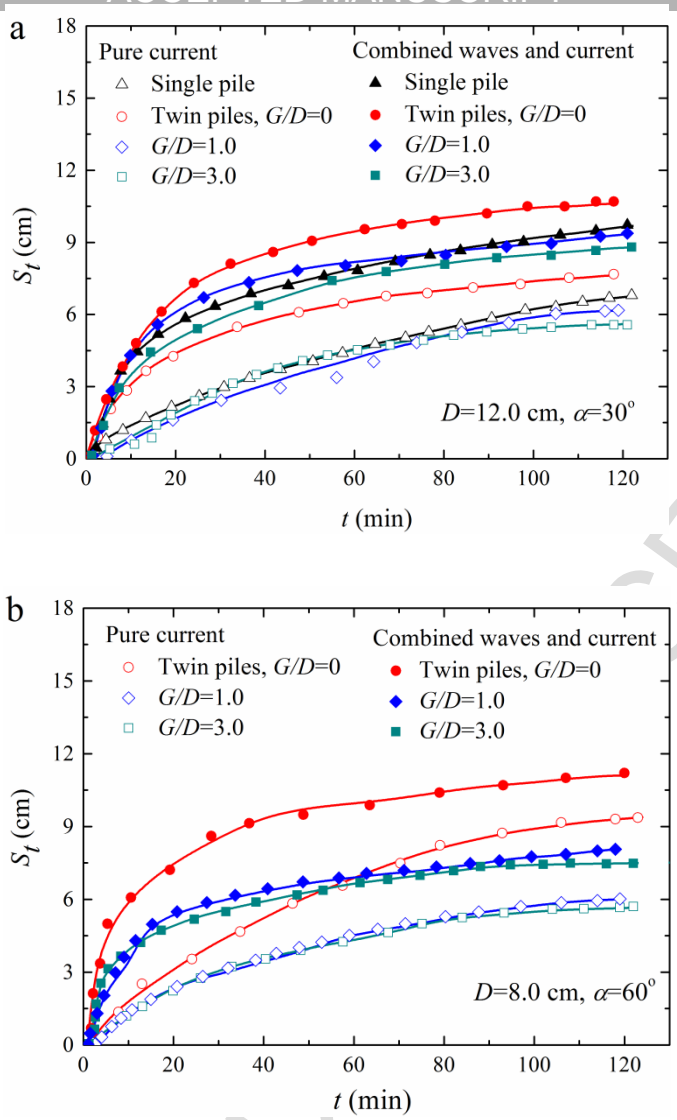

Fig. 8. Time development of scour depth measured at upstream edge of the front pile with various pile spacings for staggered arrangement: (a) α=30° (pure current: runs 1 & 5-7; combined waves and current, runs 15 & 18-20); (b) α=60° (pure current: runs 9-11; combined waves and current: runs 22-24).

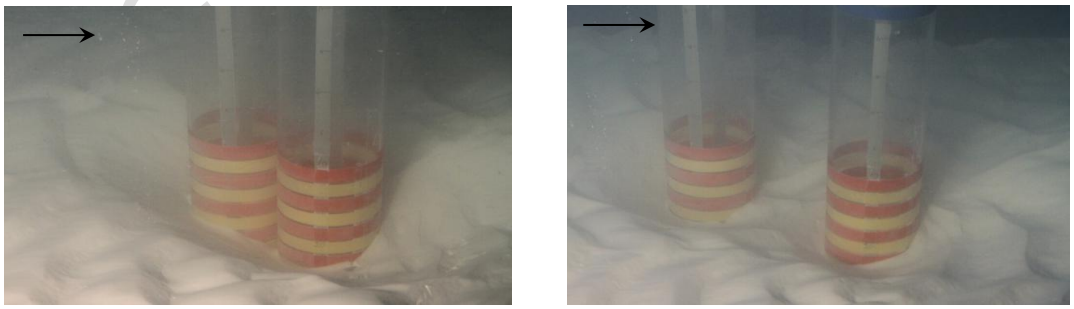

(a) (b)

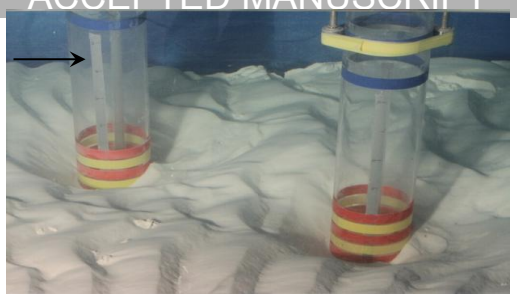

(c)

Fig. 9. Scour holes around the twin piles under combined waves and current with a flow skew angle of α=30° and pile spacing of (a) *G/D*=0; (b) *G/D*=1.0; (c) *G/D*=3.0.

Figs. 10 and 11 give the time-averaged fields of flow velocity and swirling strength at the upstream corner of twin piles with staggered arrangements (α=30° and 60°, *G/D*=0 and 1.0). By comparing Fig. 10(a) with Fig. 10(b), it can be seen that the size of the HSV for *G/D*=0 is larger than that for *G/D*=1.0 while the maximum swirling strength are generally the same. The increased size of the HSV can explain the enhanced scouring process for the case of *G/D*=0 relative to *G/D*=1.0 (α=30°, see Fig. 8). The similar comparison and conclusion also apply to Figs .11(a) and (b). The size of the HSV shown in Fig. 11(a) is much larger and the shape seems to be more irregular than that for α = 30° and *G/D*=0 shown in Fig. 10(a), impling that the HSV in Fig. 11(a) is relatively more turbulent and may oscillate in a wider range. Thus for the cases with *G/D*=0, the scouring process for α = 60° is more severe than α = 30° (see Fig. 14).

Fig. 10(c) shows that no observable HSV is detected at the rear pile for *G/D*=0 and α=30°. This is because that the location of this measurement is beyond the scope of the HSV at the front pile, meanwhile, the incoming flow is disturbed/sheltered by the front pile and no HSV can be locally formed at the rear pile. The maximum swirling strength locates at X=42 mm close to the bottom, which basically coincides with the front pile surface (refer to Fig. 4). Therefore, this very small vortex with high swirling strength could be resulted from the singularity at the side junction between pile circumference and the bottom.

In contrast to Fig. 10(c), the HSV can be clearly seen in Fig. 10(d) due to the gap between the two piles. The sizes of the HSV in Figs. 10(b) and 10(d) are generally the same as the single pile case shown in Fig. 5, while the maximum swirling strength is lower. It is noted that in Fig. 10(d), there is a band of vortices near to the bottom ahead of the HSV at the rear pile. The similar band of vortices can also be found around the rear pile for the other staggered arrangement of $\alpha = 60^{o}$ and G/D=1.0 (see Fig. 11(d)). A reasonable inference of the mechanism for this band of vortices is the interaction between the wake vortices shedding from the front pile and the bottom. This band of vortices can uplift sediment particles from the bed and thus contribute to the scouring process around the rear pile. The present scour tests indicate that the maximum scour depth always locates at the rear pile rather than the front pile for the staggered arrangements with G/D=1.0 and 3.0, which can be reasonably explained by the contribution of this band of vortices. Compared with the results of single pile case, despite the lower maximum swirling strength and generally the same sizes of the HSV, the maximum scour depths are still larger for the staggered arrangements with G/D=1.0 due to the contribution of the band of vortices (see Fig. 16).

An interesting fact is that the maximum swirling strength of the HSV at the front pile for both the staggered arrangements (Figs. 10(a), 10(b), 11(a) and 11(b)) and the tandem arrangements (Figs. 8(a) and (b)) is significantly lower than the single pile case (Fig. 5). This phenomenon indicates that the rear pile obstructing the wake vortices shedding from the front pile can reduce the swirling strength of the HSV at the front pile, even when the rear pile is totally sheltered from the incoming flow by the front pile.

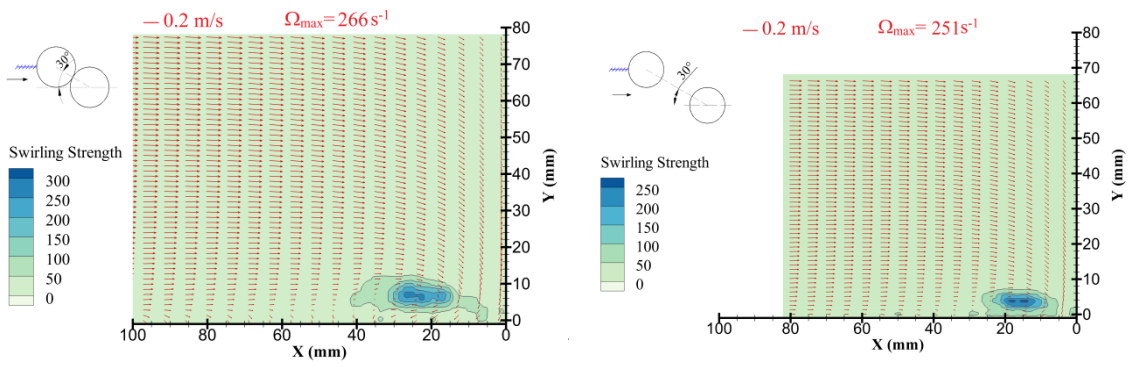

(a) (b)

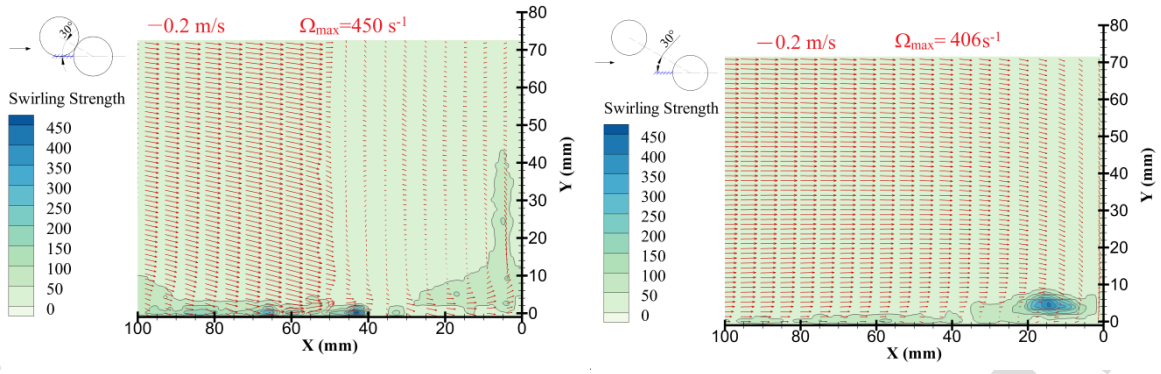

(c) (d)

Fig. 10. Time-averaged fields of flow velocity and swirling strength at the upstream corner of twin piles: (a) front pile, $\alpha = 30^{o}$, G/D=0; (b) front pile, $\alpha = 30^{o}$, G/D=1.0; (c) rear pile, $\alpha = 30^{o}$, G/D=0; and (d) rear pile, $\alpha = 30^{o}$, G/D=1.0.

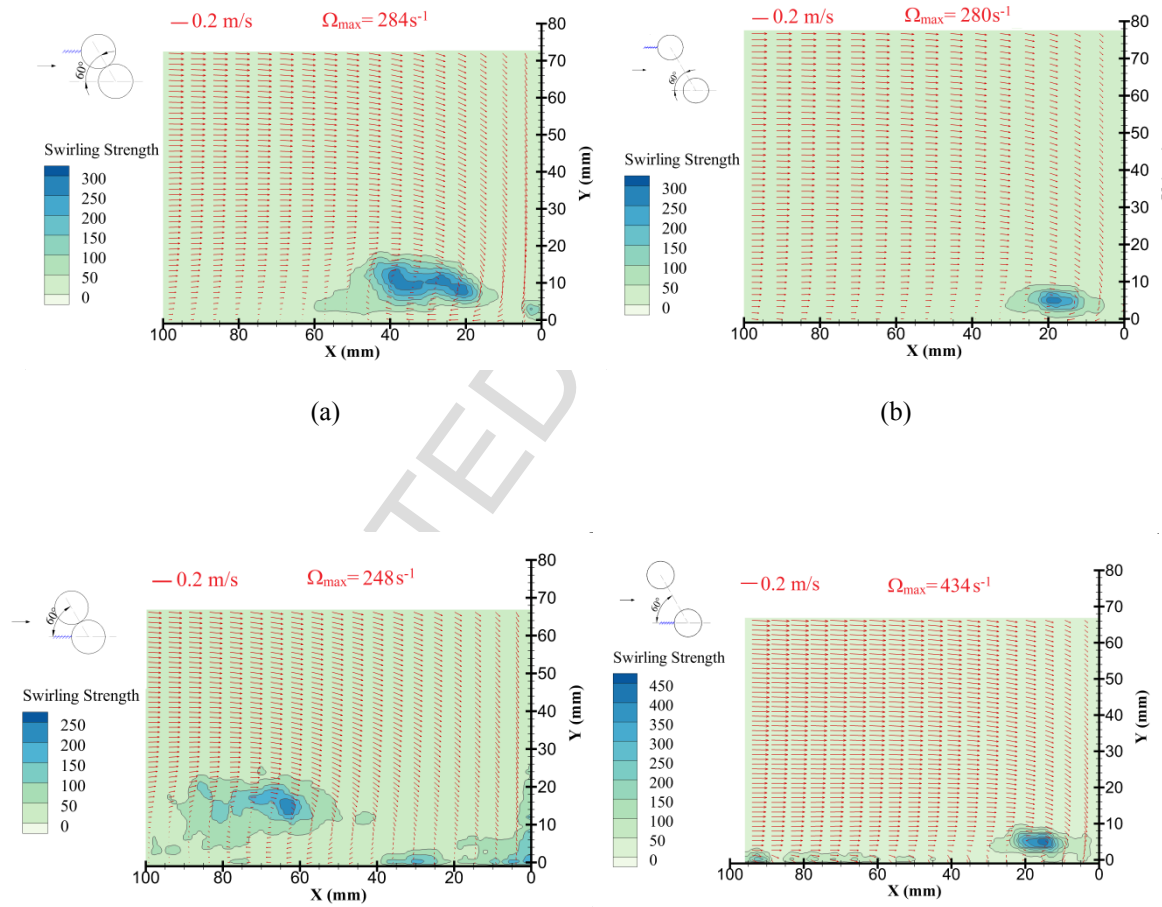

(a) (b)

(c) (d)

Fig. 11. Time-averaged fields of flow velocity and swirling strength at the upstream corner of twin piles: (a) front pile, $\alpha = 60^{o}$, G/D=0; (b) front pile, $\alpha = 60^{o}$, G/D=1.0; (c) rear pile, $\alpha = 60^{o}$, G/D=0; and (d) rear pile, $\alpha = 60^{o}$, G/D=1.0.

3.1.3 Side-by-side arrangements

For the side-by-side arrangements, the effect of pile spacing on the scour development is significant, as shown in Fig. 12. Under pure current, the initial stage of the scour depth development with a rapid increasing rate is not very much influenced by the pile spacing, whilst the development curves exhibit observable difference in the next section of approximating the equilibrium state. Under combined waves and current, the whole curves of scour depth development are distinguishable for different spacings. As the spacing increases, the pile-group effect gradually reduces.

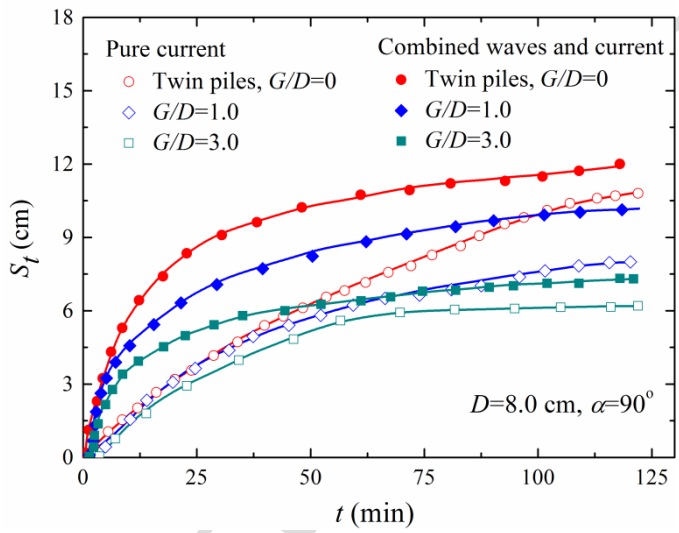

Fig. 12. Time development of scour depth measured at upstream edge of pile with various pile spacings for side-by-side arrangement (pure current: runs 12-14; combined waves and current: runs 25-27).

The time-averaged fields of flow velocity and swirling strength at the upstream corner and middle plane of twin piles with side-by-side arrangements are shown in Fig. 13. It can be seen in Figs. 13(a) and (b) that the twin piles with α=90° and G/D=0 behave as a single pile with larger diameter. The HSV is observed either at the upstream corner of each pile and middle plane of twin piles (different sections of the same HSV). The maximum swirling strength of the HSV at the twin piles with α=90° and G/D=0 is approximately 45% larger than the single pile case, inducing the largest scour depth in all the examined pile arrangements

(shown in Fig. 16). The position of the HSV core is approximately X=50 mm. Assuming the value of $\lambda_0/D = 0.17$ for the single pile case (see Fig. 5) still holds for the twin piles with α=90° and G/D=0, an equivalent diameter of D=29 cm, which is about 2.4 times of the diameter of single pile, can be deduced.

For the case with α=90° and G/D=1.0 shown in Figs. 13(c) and (d), two separate HSVs are formed at each pile. All the characteristics (size, position and maximum swirling strength) of the HSV at each pile are generally the same as the single pile case. In the middle plane between the twin piles examined in Fig. 13(d), the velocity of the incoming flow is enhanced by approximately 30% due to the blockage effect while approaching the gap. This gap flow with higher velocity could uplift and transport sediment particles, contributing to the scouring process. As such, the maximum scour depth under the condition of α=90° and G/D=1.0 occurs at the junctions between the piles and the gap, and is much larger than the single pile case (see Fig. 16).

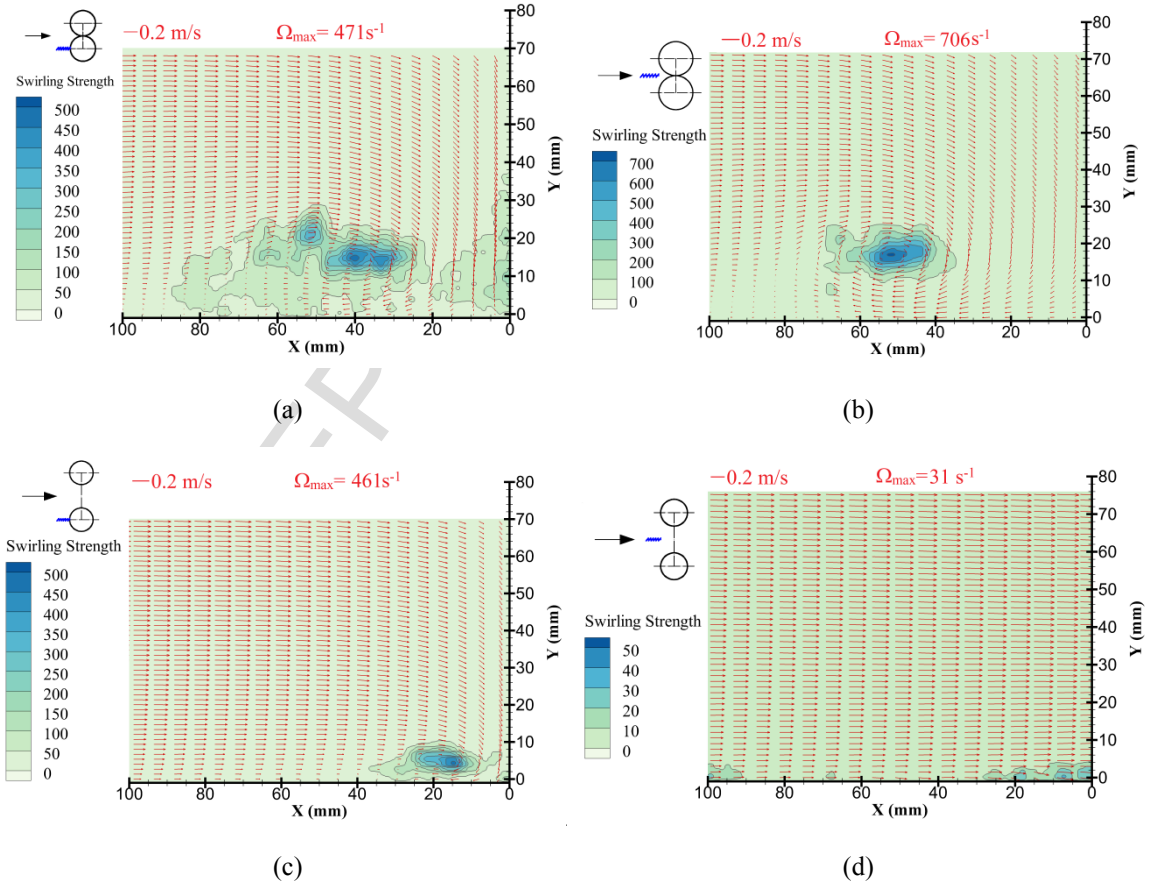

Fig. 13. Time-averaged fields of flow velocity and swirling strength at the upstream corner and middle plane of twin piles: (a) upstream corner, α = 90°, G/D=0; (b) middle plane, α = 90°, G/D=0; (c) upstream corner, α = 90°, G/D=1.0;

and (d) middle plane, $\alpha = 90^{o}$, G/D=1.0.

3.1.4 Effects of flow skew angle

The controlling mechanism for local scour around piles is the three-dimensional vortices induced by pile-current/wave interaction. For pile groups, the vortices around each single pile interact with each other and thus change the scour development around the piles. Besides the pile spacing, the flow skew angle is the other crucial parameter for determining the scour development around pile groups.

Fig. 14 gives two series of scour depth developments at the upstream edge of the front pile for various orientations and G/D=0 under pure current and combined waves and current. A comparison of the scour holes around the twin piles under pure current with various α and G/D=0 is shown in Fig. 15. Under pure current, both the scouring rate at the initial stage and the equilibrium scour depth are remarkably enhanced as the flow skew angle increases, which would be attributed to the enhanced HSV resulted from the increasing projected width of the piles onto a plane normal to the flow. Under the conditions of combined waves and current, the equilibrium scour depth is obviously increased by increasing flow skew angle, while the scouring rate at the initial stage seems to be little influenced. A comparison between pure current and combined waves and current indicates that, the effect of flow skew angle under which the live-bed condition prevails is not as obvious as that under which the clear-water condition prevails.

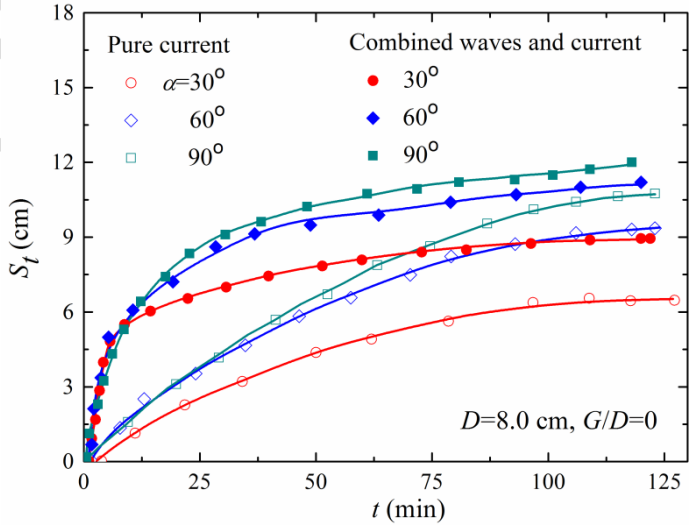

Fig. 14. Time development of scour depth measured at upstream edge of the front pile with various orientations (pure current: runs 8, 9 & 12; combined waves and current: runs 21, 22 & 25).

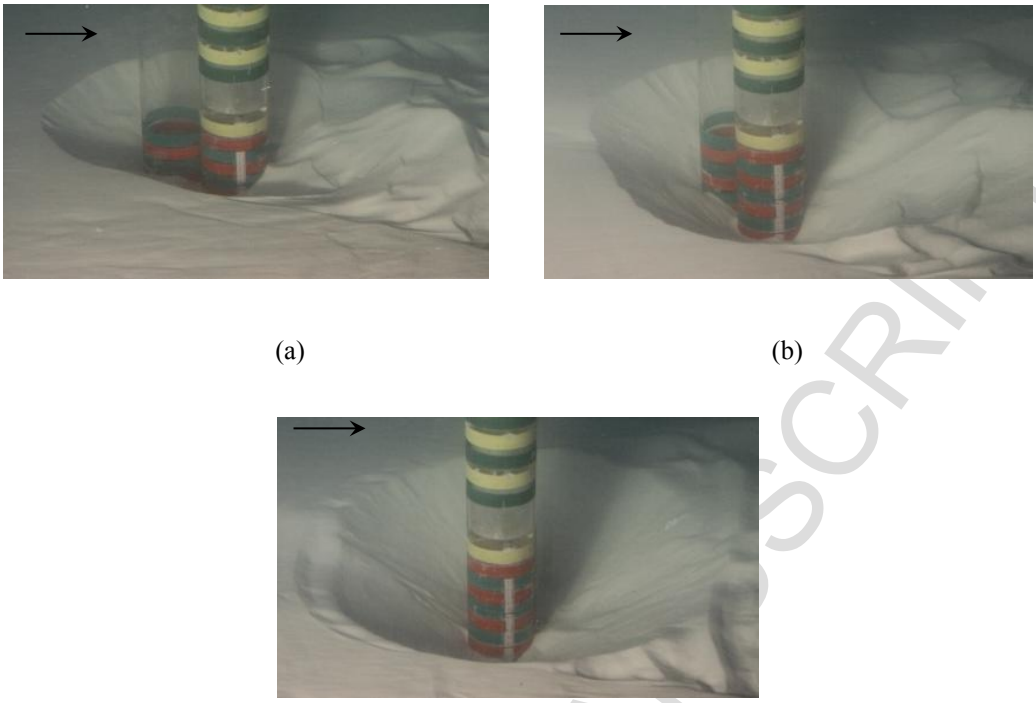

(a) (b)

(c)

Fig. 15. Scour holes around the twin piles under pure current with a pile spacing of G/D=0 and flow skew angle of (a) α=30°; (b) α=60°; (c) α=90°.

3.1.5 Time scale of scour

The time scale of scour process is a certain amount of elapsed time for a substantial amount of scour to develop (Sumer and Fredsøe, 2002), which is essential for predicting the scour depth at any instant in a certain wave and/or current condition. The time scale of scour process can be defined in several ways according to different mathematical functions for approximating the scour development towards the equilibrium stage. For example, the following definition is proposed by Sumer et al. (1992a):

$$S_t = S_e\left(1-\exp\left(-\frac{t}{T_0}\right)\right) \tag{7}$$

where S_e is the equilibrium scour depth and T_0 is a constant to define the time scale. Alternatively, Briaud et

al. (1999) proposed following hyperbolic function:

$$S_t = S_e \frac{t}{t + T_0} \tag{8}$$

For the present measured scour development, a comparison indicates that the hyperbolic function expressed with Eq. (8) performs better than the exponential function expressed with Eq. (7). Therefore, Eq. (8) was utilized to approximate the measured scour developments (see Figs. 6, 8 and 12) and further estimate the time scale of scour in this paper.

The non-dimensional time scale for pure current cases and combined wave-current cases is presented in Fig. 16 (a) and (b), respectively. The non-dimensional time scale T_0^* is calculated by

$$T_0^* = T_0 \frac{\left(g\left(s-1\right)d_{50}^3\right)^{\frac{1}{2}}}{D^2} \tag{9}$$

Distinctive variation trends of T_0^* with flow skew angle can be seen between pure current cases and combined wave-current cases.

For pure current cases shown in Fig. 16(a), the time scale of scour reaches a minimum value at an intermediate flow skew angle of α=30°. The effect of pile spacing on the time scale seems not obvious for α=0° and 30°. Nevertheless, for α=0° and 30°, the decrease of T_0^* can be consistently observed with increasing G/D. When G/D=3.0, T_0^* has the similar value to the case of single pile (T_0^*=0.19 for single pile under pure current) and the pile group effect on the time scale is considered negligible.

With respect to the cases under combined waves and current shown in Fig. 16(b), T_0^* increases nearly linearly with increasing flow skew angle for a fixed value of G/D. The time scale for G/D=1.0 is generally larger than G/D=0. An interesting observation from Fig. 16(b) is that the time scale under combined waves and current is till remarkably influenced by flow skew angle for G/D=3.0. When α=90° and G/D=3.0, T_0^* is significantly larger than the case of single pile (T_0^*=0.04 for single pile under combined waves and current),

indicating a prominent pile-group effect. This is very unlike the pile-group effect on the maximum scour depth (generally vanishing for $G/D \geq 3.0$; see Section 3.2) and on the time scale for pure current cases. Recalling that the time scale is essentially a measure of the time for a substantial amount of scour to develop, T_0^* has a positive correlation with the ratio of the scour hole volume to the local sediment transport rate. Since the maximum scour depth around twin piles S approximates that around a single pile (see Section 3.2) and the scour hole volume is generally proportional to S^3, a reduced local sediment transport rate is inferred to be the controlling mechanism for the enhanced T_0^* for α=90° and G/D=3.0. Additional experimental evidence is in need for this explanation.

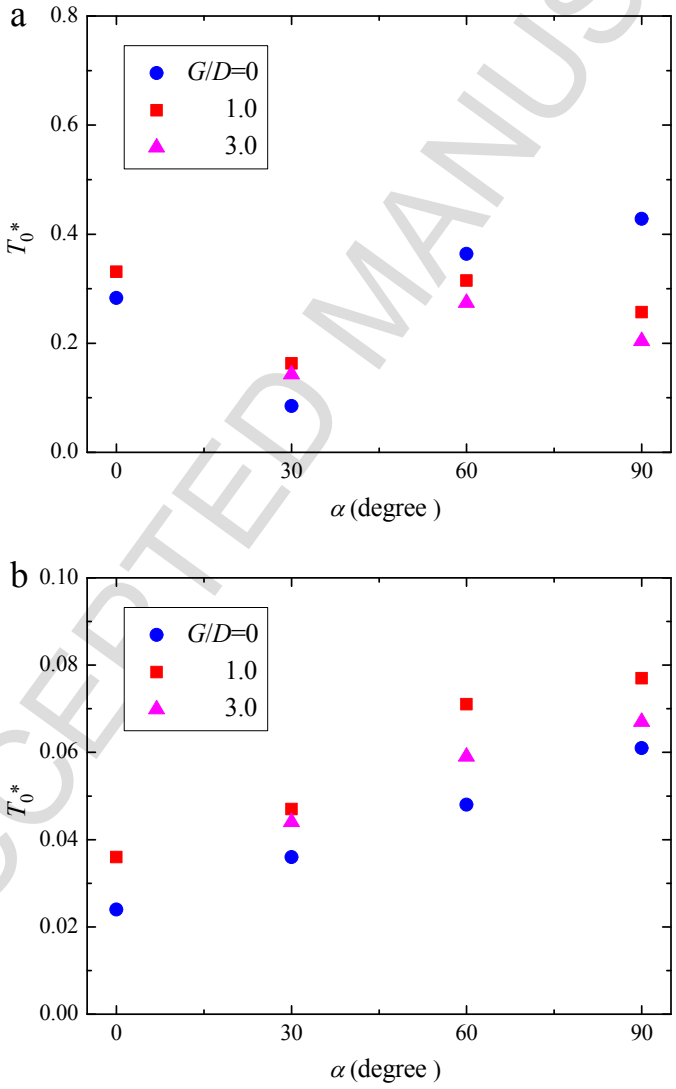

Fig. 16. The non-dimensional time scale of scour process around twin piles: (a) pure current under clear-water regime; and (b) combined waves and current under live-bed regime.

3.2. Maximum scour depth

The variations of the present measured maximum scour depth around twin piles with pile spacing are plotted in Fig. 17. The observed maximum scour depth at time t=120 min was used as the equilibrium scour depth (refer to Qi and Gao, 2014b). To focus on the pile-group effect, the maximum scour depth is normalized by the scour depth around a single pile (S_0) under the same hydrodynamic condition. Note that the maximum scour depth around twin piles is not necessarily at the upstream edge of the front pile, but vary its position according to the pile arrangement and hydrodynamic condition.

Fig. 17 shows that S/S_0 gradually approaches the value of S/S_0=1.0 with increasing spacing, implying that the pile-group effect on the maximum scour depth almost disappears when G/D=3.0. For the cases with α=0° and G/D=0, the value of S/S_0 is by and large smaller than 1.0, indicating that the pile-group effect could reduce the scour depth in this scenario. In contrast, large flow skew angle is always beneficial to enhancing the maximum scour depth. The most significant pile-group effect emerges for side-by-side arrangements (α=90°). As an extreme example, for the condition of α=90° and G/D=0, the value of S/S_0 can be up to approximately 2.1, which is also more than the scour depth around a single 16.0 cm pile under the same flow conditions. As explained by Liang et al. (2013), this is because the geometry of the twin piles is less streamlined and thus induces larger adverse pressure gradient, earlier boundary layer separation, and more intensive vortices (also see Fig. 13). In the practical offshore environments, the flow skew angle could be diverse and thus the upper envelope of S/S_0 with G/D under α=90° is of great significance.

Under the condition of α=0° and α=30°, the variation curves of S/S_0 with G/D are generally consistent for both pure current and combined waves and current. That is, the enhancement of the maximum scour depth due to pile-group effect seems to be uninfluenced by the flow condition (clear-water condition for pure current, live-bed condition for combined waves and current) for relatively small flow skew angle (e.g. $\alpha \leq$30°). In contrast, under the condition of α=60° and α=90°, the variation curves of S/S_0 with G/D for live-

bed condition (combined waves and current) distribute remarkably above those for clear-water condition (pure current). The value of S/S_0 for live-bed condition can be larger than clear-water condition by approximately 30% for α=60° and α=90°.

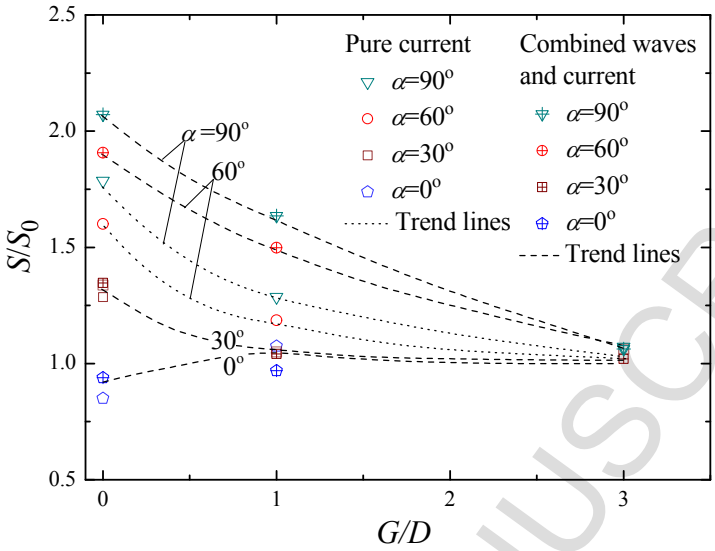

Fig. 17. Variation of S/S_0 with pile spacing.

Fig. 18 gives the comparison of the maximum scour depth between the present measured data and the existing experimental data. It can be seen from Fig. 18(a) that for the tandem pile arrangement (α=0°), the holistic variation trends of S/S_0 with G/D are the same in spite of different incipient flow and soil conditions. Nevertheless, the specific values of S/S_0 hold considerable deviation between different tests. For the side-by-side arrangement (α=90°) shown in Fig. 18(b), the present results under pure current agree very well with the preceding data. The pile-group effect is obvious for G/D<3 and gradually vanishes for G/D≥3. The values of S/S_0 for combined waves and current are obviously larger than those for the pure current. This unfavorable effect should be taken into consideration while evaluating the scour depth around group piles in marine environments. As an example, a safety factor of 1.3 can be multiplied to the estimated scour depth under pure current.

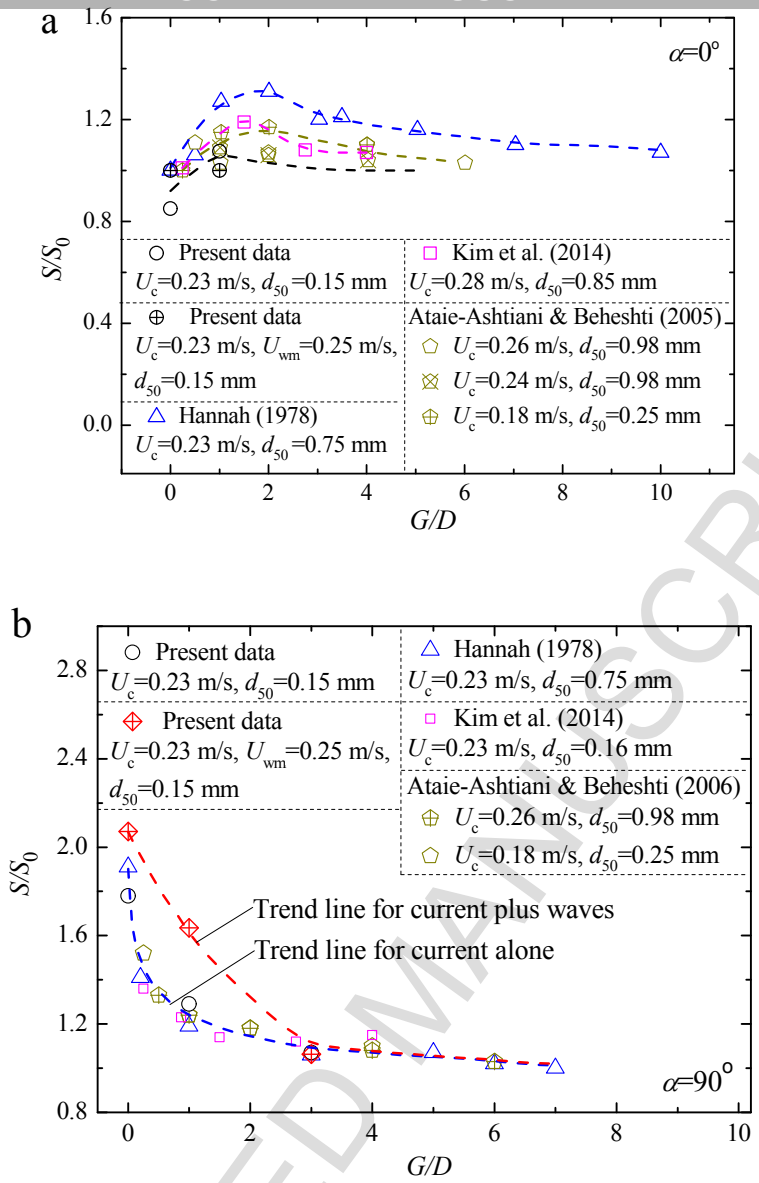

Fig. 18. Comparison of the maximum scour depth between the present measured data and the existing experimental data: (a) α=0°; (b) α=90°.

3.3. Equivalent pile diameter

To incorporate the pile-group effect into the evaluation of the maximum scour depth at twin piles, a parameter of "equivalent pile diameter" D^* is introduced. The equivalent pile diameter is a modification of the single pile diameter according to the pile spacing G/D and flow skew angle α. The concept of D^* is established on the assumption that the influence of the other pile on the flow field and resulting maximum

scour depth around the target pile can be equated to the effect of increasing/decreasing the single pile diameter. By adopting the equivalent pile diameter, the trend curves in Fig. 17 are expected to be uniformly described.

The empirical formula of D^* expressed by G/D and α can be obtained according to the present and existing data using the least square method. For the cases with pure current (clear-water condition), the following equation proposed by Zanke et al. (2011) is adopted

$$S/D = 2.5\left(1-0.5U_{cr}/U\right)x_{rel} \tag{10}$$

in which U is the mean velocity in case of steady currents, and x_{rel} is a parameter for describing the transition between the extremes of pure current and pure waves (x_{rel} =1 for the examined cases of pure current here). U_{cr} is the critical velocity for initiation of sediment motion and is expressed as $U_{cr} = 1.4\left(2\sqrt{\frac{\rho_s-\rho_w}{\rho_w}gd_{50}}+10.5\frac{\nu}{d_{50}}\right)$. The values of D^*/D can be obtained by substituting the measured value of S/S_0, U, and the calculated value of U_{cr} into Eq. (10).

With respect to the maximum scour depth around a pile under combined waves and current (live-bed condition), an empirical model of equilibrium scour depth was established (Qi and Gao, 2014a)

$$\lg(S/D) = -0.80\exp\left(0.14/Fr_a\right)+1.11 \qquad \text{(live-bed; } 0.1<Fr_a<1,\ 0.4<KC<26\text{)} \tag{11}$$

The expression of Fr_a is given in Eq. (3). By adopting the average water particle velocity during one-quarter cycle of oscillation under combined waves and current U_a in the definition, Fr_a is correlated with the scale of the HSV, and thus relates to the scouring process. Eq. (11) performs well in terms of the lab data spanning several experimental studies. A preliminary and straightforward estimate of scour depth should be feasible using Eq. (11), albeit acknowledging its oversimplification with respect to wave parameters (e.g. wave period). For the combined wave-current cases under live-bed regime, the values of D^*/D can be deduced by substituting the measured maximum scour depth around twin piles S and the calculated value of Fr_a into Eq. (11).

Based on the acquired data of D^* corresponding to various G/D and α (in rad), the following formula for

the dimensionless equivalent pile diameter is derived

$$D^*/D=\left[1+1.04\left(\sin\alpha\right)^{1.24}\exp\left(-0.68\,G/D\right)\right] \tag{12}$$

It should be noted that this expression is only verified for the pure current cases in clear-water regime and the combined wave-current cases in live-bed regime, with limited experimental data points. Application of Eq. (12) should be conducted with due caution and further validation.

The variations of D^*/D with G/D and α according to Eq. (9) are displayed in Fig. 19. It is indicated that with increasing G/D and decreasing α, the value of D^*/D gradually approaches 1.0 and pile-group effect vanishes. The peak value of $D^*/D\approx2.04$ occurs when $G/D=0$ and $\alpha=90^o$, implying that in terms of local scour, the side-by-side twin piles without gap approximately acts like a single pile with diameter equal to the projected width onto a plane normal to the flow.

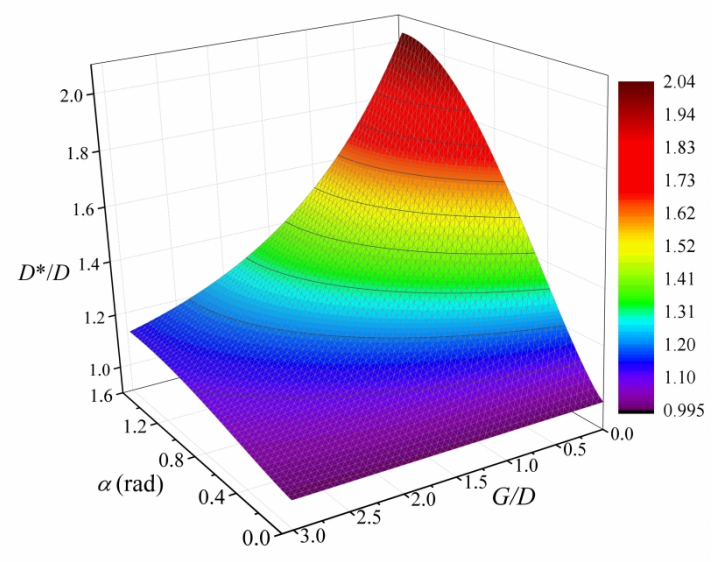

Fig. 19. Variations of D^*/D with G/D and α.

The feasibility of Eq. (12) is evaluated by comparing the measured values of S/S_0 with the calculated ones based on Eqs. (10)-(12) (see Fig. 20). It is indicated that 90% of the data distribute in the range of 20% error lines and all the data are within the range of 25% error lines for either the pure current cases under clear-water regime or combined waves and current cases under live-bed regime.

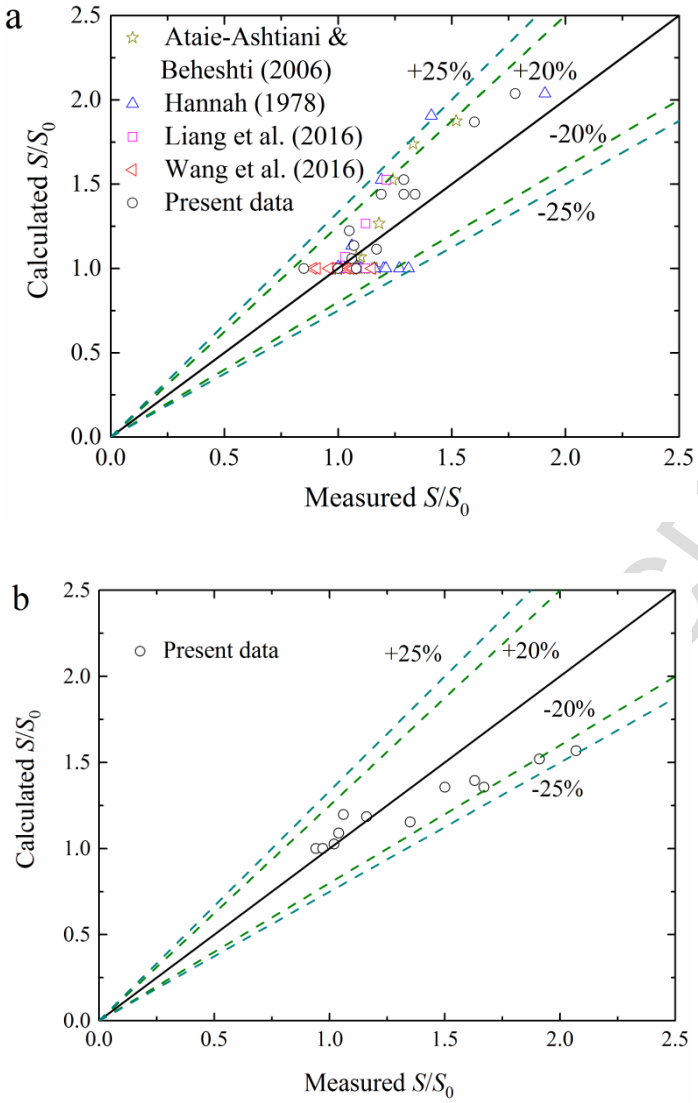

Fig. 20. Comparison of the measured and predicted values of S/S_0: (a) pure current under clear-water regime; and (b) combined waves and current under live-bed regime.

4. Conclusions

Local scour around piles in marine environments can significantly compromise the stiffness and bearing capacity of pile foundations for coastal and offshore structures. Different from the scour around the monopile (single pile) foundation, the local scour at pile groups is a complicated process, involving more influential factors. Pile group effects are examined by physical modeling with a series of large flume tests on twin piles. Besides the pure current condition, the local scour around twin piles under combined waves and current was

intensively investigated. The following conclusions can be drawn.

(1) The experimental observations indicate that the pile-group effect is obvious for $G/D<3.0$ and gradually vanishes for $G/D\geq3.0$. The influence of pile spacing on the scour depth development is much more significant for the side-by-side ($\alpha=90^{o}$) arrangement than that for the tandem arrangement ($\alpha=0^{o}$). The maximum swirling strength of the HSV at side-by-side twin piles without gap ($\alpha=90^{o}$, $G/D=0$) is approximately 45% larger than the single pile case, inducing the largest scour depth in all the examined pile arrangements. In contrast, the maximum swirling strength of the HSV for tandem arrangements is significantly lower than the single pile case, which could be responsible for the reduced maximum scour depth for tandem arrangements compared to the single pile case. With the increase of flow skew angle α, the maximum scour depth is remarkably enhanced within the examined range $0\leq G/D\leq3.0$.

(2) Under the condition of pure current with side-by-side arrangements, there is a good agreement between the present measured maximum scour depth and the previous results. This consistent upper envelope of S/S_0 with G/D under pure current is of great significance for considering the diverse flow skew angle in the practical marine environments. In terms of the effect of hydrodynamic condition, the variation curves of S/S_0 with G/D are generally consistent for both pure current and combined waves and current, under the condition of $\alpha=0^{o}$ and $\alpha=30^{o}$. In contrast, the values of S/S_0 for combined waves and current can be larger than those for pure current by approximately 30% for $\alpha=60^{o}$ and $\alpha=90^{o}$. Such effect of large flow skew angles should be taken into consideration while evaluating the scour depth around group piles in marine environments.

(3) An equivalent pile diameter D^{*}, which is a modification of the single pile diameter according to the pile spacing and flow skew angle, is introduced to incorporate the pile-group effect into the evaluation of the maximum scour depth at twin piles. An empirical formula of the dimensionless equivalent pile diameter expressed by G/D and α is established on the basis of the existing experimental data. A comparison between

the measured values of S/S_0 and the calculated ones based on the empirical formula of D^* shows that, 90% of the data distribute within the range of 20% error lines and all the data are within the range of 25% error lines for either the pure current cases or the combined waves and current cases.

Acknowledgements

This work is financially supported by the National Natural Science Foundation of China (Grant No. 11602273), the Major State Basic Research Development Program of China (973 Program) (Grant No. 2014CB046204) and the Youth Innovation Promotion Association CAS. The authors would also like to thank the anonymous reviewers for constructive comments and suggestions for improvement of the final manuscript.

References

[1] Anderson, C.D., Lynch, S.P., 2016. Time-resolved stereo PIV measurements of the HSV system at multiple locations in a low-aspect-ratio pin–fin array. Experiments in Fluids 57(1), 1-18.

[2] Ataie-Ashtiani, B., Beheshti, A., 2006. Experimental investigation of clear-water local scour at pile groups. Journal of Hydraulic Engineering 132(10), 1100-1104.

[3] Ballio, F., Bettoni, C., Franzetti, S., 1998. A survey of time-averaged characteristics of laminar and turbulent horseshoe vortices. Journal of Fluids Engineering 20, 233-242.

[4] Bayram, A., Larson, M., 2000. Analysis of scour around a group of vertical piles in the field. Journal of Waterway, Port, Coastal and Ocean Engineering 126(4), 215-220.

[5] Briaud, J.L., Ting, F.C.K., Cheng, H.C, Gudavalli, R., Perugu, S., Wei, G.S., 1999. SRICOS: prediction of scour rate in cohesive soils at bridge piers. Journal of Geotechnical and Environmental Engineering 125(4), 237-246.

[6] Chiew, Y.M., Melville, B.W., 1987. Local scour around bridge piers. Journal of Hydraulic Research 25(1), 15-26.

[7] Chong, M.S., Perry, A.E., Cantwell, B.J., 1990. A general classification of three-dimensional flow field. Physics of Fluids A(2):765-777.

[8] Hannah, C.R., 1978. Scour at pile groups. University of Canterbury, N.Z., Civil Engineering, Research

Report No. 78-3:92.

[9] Kim, H.S., Nabi, M., Kimura, I., Shimizu, Y., 2014. Numerical investigation of local scour at two adjacent cylinders. Advances in Water Resources 70, 131-147.

[10] Kirkil, G., Constantinescu, G., 2015. Effects of cylinder reynolds number on the turbulent HSV system and near wake of a surface-mounted circular cylinder. Physics of Fluids 27(7), 477-539.

[11] Larsen, B.E., Fuhrman, D.R., Baykal, C., Sumer, B.M. 2017. Tsunami-induced scour around monopile foundations. Coastal Engineering 129, 36-49.

[12] Liang, D., Gotoh, H., Scott, N., Tang, H., 2013. Experimental study of local scour around twin piles in oscillatory flows. Journal of Waterway, Port, Coastal and Ocean Engineering 139(5), 404-412.

[13] Liang, F., Wang, C., Huang, M., Wang, Y., 2016. Experimental observations and evaluations of formulae for local scour at pile groups in steady currents. Marine Georesources & Geotechnology.

[14] Melville, B.W., Chiew, Y.M., 1999. Time scale for local scour in bridge piers. Journal of Hydraulic Engineeering 125, 59–65.

[15] Muzzammil, M., Gangadhariah, T., 2003. The mean characteristics of HSV at a cylindrical pier. Journal of Hydraulic Research 41(3), 285-297.

[16] Myrhaug, D., Rue, H., 2005. Scour around group of slender vertical piles in random waves. Applied Ocean Research 27(1), 56–63.

[17] Qi, Y., Xiao, W., Yue, D.K.P., 2016. Phase-resolved wave field simulation calibration of sea surface reconstruction using noncoherent marine radar. Journal of Atmospheric and Oceanic Technology, 33(6), 1135-1149.

[18] Qi, W.G., Gao, F.P., 2014a. Equilibrium scour depth at offshore monopile foundation in combined waves and current. Science China Technological Sciences 57(5), 1030-1039.

[19] Qi, W.G., Gao, F.P., 2014b. Physical modeling of local scour development around a large-diameter monopile in combined waves and current. Coastal Engineering 83, 72-81.

[20] Sheppard, D.M., Odeh, M., Glasser, T., 2004. Large scale clear-water local pier scour experiments. Journal of Hydraulic Engineering 130(10), 957-963.

[21] Soulsby, R., 1997. Dynamics of Marine Sands. Thomas Telford, UK.

[22] Sumer, B.M., Christiansen, N., Fredsoe, J., 1992a. Time scale of scour around a vertical pile. Proceedings of The Second International Offshore and Polar Engineering Conference, San Francisco,

308-315.

[23] Sumer, B.M., Christiansen, N., Fredsøe, J., 1997. The horseshoe vortex and vortex shedding around a vertical wall-mounted cylinder exposed to waves. Journal of Fluid Mechanics 332, 41-70.

[24] Sumer, B.M., Fredsøe, J., 1998. Wave scour around group of vertical piles. Journal of Waterway, Port, Coastal and Ocean Engineering 124, 248-256.

[25] Sumer, B.M., Fredsøe, J., 2002. The Mechanics of Scour in the Marine Environment. World Scientific. Singapore.

[26] Sumer, B.M., Fredsøe, J., Christiansen, N., 1992b. Scour around a vertical pile in waves. Journal of Waterway, Port, Coastal and Ocean Engineering ASCE, 118(1), 15-31.

[27] Wang, H., Tang, H., Liu, Q., Wang, Y., 2016. Local scouring around twin bridge Piers in open-channel flows. Journal of Hydraulic Engineering 142(9), 06016008.

[28] Whitehouse, R., 1998. Scour at Marine Structures: a Manual for Practical Applications. Thomas Telford, London.

[29] Yagci, O., Yildirim, I., Celik, M.F., Kitsikoudis, V., Duran, Z., Kirca, V.O., 2017. Clear water scour around a finite array of cylinders. Applied Ocean Research 68, 114-129.

[30] Zang, Z.P., Gao, F.P., Cui, J.S., 2013. Physical modeling and swirling strength analysis of vortex shedding from near-bed piggyback pipelines. Applied Ocean Research 40(3), 50-59.

[31] Zanke, U.C.E., Hsu, T.W., Roland, A., Link, O., Diab, R., 2011. Equilibrium scour depths around piles in noncohesive sediments under currents and waves. Coastal Engineering 58(10), 986-991.

Notation

The following symbols are used in this paper:

d seabed depth
d_{50} median diameters of soil
D pile diameter
D_r relative density of soil
D_* dimensionless grain size
Fr pile Froude number
Fr_a average-velocity based pile Froude number
g gravitational acceleration
G distance between two piles
h water depth
H wave height
KC Keulegan-Carpenter number
n soil porosity
Re pile Reynolds number
s specific gravity of sand grains
S maximum scour depth around twin piles
S_0 maximum scour depth around a single pile
S_e equilibrium scour depth
S_t scour depth at any instant
t time
T wave period
T_0 time scale of scour
T_0^* normalized time scale of scour
U_a average water particle velocity during one-quarter cycle of oscillation under combined waves and current, when the oscillatory motion and the current are in the same direction
U_c representative near-bed velocity of the current component of the undisturbed combined flow
U_{cr} critical velocity for initiation of sediment motion
U_f maximum value of the undisturbed friction velocity
U_m maximum value of the combined waves and current velocity at the level of $1.0D$ above the sand-bed.
U_{wm} maximum velocity of the undisturbed wave-induced oscillatory flow at the level of $1.0D$ above the sand-bed
x horizontal coordinate
y vertical coordinate
α flow skew angle
γ' submerged unit weight of soil
θ Shields parameter
θ_{cr} critical Shields parameter for sediment incipient motion
ρ_s sediment grain density
ρ_w water density
σ_g geometric standard deviation of soil grains
λ_0 longitudinal coordinates with the intersection point between the upstream pile edge and the bed surface being set as the origin

ν kinematic viscosity of water

ξ_v vertical coordinates with the intersection point between the upstream pile edge and the bed surface being set as the origin

Ω_{max} maximum swirling strength

Highlights:

- ✧ Flume modelling of local scour at twin piles under pure-current and combined wave-current was conducted to investigate the effects of pile spacing and flow skew angle;
- ✧ Flow measurements around twin piles under pure current were carried out using PIV technique to reveal the mechanism for pile-group effects;
- ✧ Empirical formula for evaluating the maximum scour depth around twin piles is proposed by introducing an equivalent pile diameter.